Mode Selection and Power Optimization for Energy Efficiency in Uplink Virtual MIMO Systems

Yun Rui, Q. T. Zhang, *Fellow, IEEE*, Lei Deng, Peng Cheng, Mingqi Li

***Abstract*—Driven by green communications, energy-efficient transmission is becoming an important design criterion for wireless systems, aiming to extend the life cycle of batteries in mobile devices. In this paper, we tackle the energy efficiency (EE) issue in uplink virtual multiple-input multiple-output (MIMO) systems, which requires the optimization of two interlaced parameters: the number of constituent mobile users in the virtual MIMO and their corresponding power allocation. The former parameter is a *structural* parameter defining the size of the virtual MIMO (usually known as the transmission mode) and its optimization relies on the method of enumeration. The difficulty is further aggravated by the fact that the EE is a non-convex function of power, even for a given transmission mode. By exploiting the fact that increasing the number of active users can increase the number of contributors to the total EE on one hand but reducing the diversity order for each single user on the other, we can show the existence of an optimal transmission mode and find a simple way for its search. Through in-depth analysis, we show the existence of a unique globally optimal power allocator for the case without power constraints under the assumption of zero-forcing receivers, and further reveal the impact of power constraints upon power allocation, as compared to its global counterpart, aiming to provide a powerful means for power-constrained EE optimization. Finally, we establish theories, for isometric networks, to narrow down the search range for possible transmission modes, leading to a significant reduction of computational complexity in optimization. Simulation results are presented to substantiate the proposed schemes and the corresponding theories.**

***Index Terms*—Virtual MIMO, Energy Efficiency, Mode Selection, Power Allocation**

I. Introduction

MULTIPLE-input multiple-output (MIMO) technology has attracted great attention due to its high spectral efficiency (SE). However, the application of MIMO uplink is often limited by the difficulty in practical implementation of multiple power amplifiers at users, especially in small hand-sets. To solve this problem, virtual MIMO (V-MIMO) transmission is proposed for the uplink [1] [2], which allows several users, each of a single transmit antenna, to share the same time-frequency resource blocks.

In wireless communications, SE is often a central issue and systems are thus designed for its maximization, without taking into account the power efficiency. A possible consequence is that the goal of SE maximization is indeed achieved but the system operates with the full power over a long period, resuting in deficiency in energy usage. Energy saving is a global trend today [3] [4], and the design philosophy must change accordingly. Facing this challenge, energy efficiency (EE) becomes increasingly important for mobile communications to prolong the life cycle of batteries. Physically, EE represents the exhange rate between energy and data speed, measured by the number of information bits that can be reliably conveyed over the channel per-unit energy consumption [5].

Recently, energy-efficient system design has received much attention in academia. Power-control optimization for single-antenna systems to operate on uplink code division multiple access (CDMA) Gaussian channels is tackled in the framework of game theory to maximize the individual energy efficiency of each user [6] [7]. Its counterpart for multi-carrier systems with orthogonal frequency-division multiplexing (OFDM) transmission is studied in [8], taking into account the circuit power consumption, link adaptation, and resource allocation. The case with multi-user interference is also investigated therein [9].

In contrast to its high spectral efficiency, a MIMO system can have lower energy efficiency than a single-input and single output (SISO) system [10]. A key technology to improve the EE of MIMO systems is the use of adaptive techniques. In [11], adaptive switching between MIMO and single-input and multiple-output (SIMO) is adopted to save energy at mobile terminals. For sensor networks, single-antenna terminals can cooperate among each other to form a cooperative V-MIMO system which, when used alongside space time block codes (STBC) and adaptive clustering, offers a high EE [12]. By integrating adaptive modulation and adaptively choosing spatial transmission modes for MIMO systems, the EE can be significantly improved, achieving up to 30% improvement over its non-adaptive alternative [13]. However, the operation of adaptive schemes relies on the instantaneous channel state information (CSI), and thus requires a base station (BS) to schedule huge *instantaneous CSI feedback* from multiple users. Further, there is no explicit mode switching point obtained that related to the system parameters, leading to a large overhead and a significant drop in system efficiency, which is not desirable for system in large number of users [14].

Manuscript received April 10, 2012; revised November 6, 2012. Part of this paper was presented at ICC'13.

Y. Rui is with Shanghai Advanced Research Institute, Chinese Academy of Sciences, and The State Key Laboratory of Integrated Services Networks (ISN), China (e-mail:ruiy@sari.ac.cn).

Q. T. Zhang is with the Department of Electronic Engineering, City University of Hong Kong, Hong Kong (e-mail: qtzhang@ieee.org).

L. Deng and P. Cheng are with the Department of Electronic Engineering, Shanghai Jiao Tong University, China (e-mail: {dl0729, cp2001cp}@sjtu.edu.cn). Currently, Peng Cheng is also with the CSIRO ICT Centre, Marsfield NSW 2122, Australia.

M. Li is with Shanghai Advanced Research Institute, Chinese Academy of Sciences, China (e-mail: limq@sari.ac.cn).

Digital Object Identifier 10.1109/JSAC.2013.130511.

Most existing work on energy-efficient transmission is focused on point-to-point single user transmission [8] [10]. Multi-user energy efficiency is recently considered in [9] where the CSI exchange between the users and the BS is required for a distributive decision in the framework of game-theoretic optimization. As well known, virtual MIMO is advocated in the Long Term Evolution (LTE) documents [1], expecting a simple scheduler at the BS and energy-efficient transmission for all users. Therefore in this paper, we consider the optimization issue of energy efficient uplink V-MIMO transmission, based merely on *statistical channel state information* (SCSI). The optimization includes two interlaced aspects, determining the optimal number of constituent (i.e., active) users in the V-MIMO and its corresponding optimal power allocation. The former parameter is a *structural* one of the V-MIMO while the latter is a usual system vector parameter but can be optimized only after the former is determined. The optimal number of constituent users is influenced by the channel SCSI and signal-to-noise ratio (SNR) and thus varies with the channel operating conditions and the particulars of the constituent users. As such, an energy-efficient V-MIMO system usually operates in a switching mode. Just as any MIMO system, CSI is required for coherent reception to fully exploit the MIMO channel capacity, regardless of the configuration of the receiver as V-BLAST (vertical-Bell laboratories layered space-time), ZF (zero forcing), or MMSE (minimum mean square error). The same is true for the V-MIMO addressed in this paper. Such a V-MIMO system allows each user to utilize the *full* temporal-frequency channel resource, the advantage achieved at the cost of perfect CSI available at the base station.

In this paper, we first establish the existence of global solution, and then derive efficient optimization techniques for V-MIMO systems with and without a power constraint. To reduce complexity in transmission mode adaptation, we further derive an efficient suboptimal strategy and theory for mode selection, in the context of isometric networks (which means that each user has a equal distance apart from a base station and thus their path loss are identical).

The rest of the paper is outlined as follows. The system model is described in Section II. In section III, we analyze the existence of optimal solutions to EE transmission with and without a power constraint, and subsequently develop efficient techniques for their search. We then, in Section IV, propose a spectral-efficiency based low-complexity scheme for pre-selection of the number of active users. The theory is examined in Section V through simulations, followed by concluding remarks in Section VI. Throughout the paper, we will use $\mathbf{E}[\cdot]$ to denote expectation, $\mathbf{I}$ to denote the identity matrix, and the superscript † denotes Hermitian transposition.

II. System Model

Consider the uplink transmission in which U mobile users within a cell communicate with the Node-B in a quasi-static Rayleigh flat-fading environment. We denote the set of U users as $\mathcal{U} = \{1, 2, \cdots, U\}$. Each user is assumed to employ only one transmit antenna, i.e., $N_t = 1$, while the Node-B is equipped with r receive antennas. The scheduler in the Node-B randomly selects $u \leq U$ users, from the total of U, to share the same time-frequency resource, forming a V-MIMO system characterized by an $r \times u$ channel matrix $\mathbf{H}$. Denote the set of selected u users as $\mathcal{B} = \{b_1, b_2, \cdots, b_u\} \subseteq \mathcal{U}$. To facilitate the notation in the rest of paper, we just map index i to the selected user b_i, i.e., $\mathcal{B}' = \{1, 2, \cdots, u\}$.

After appropriately power loaded with a loading matrix $\mathbf{P}_u^{1/2} = \text{diag}\{\sqrt{P_1}, \cdots, \sqrt{P_u}\}$, the symbol vector $\mathbf{s} \in \mathcal{C}^{\mathbf{u}\times\mathbf{1}}$ from the u selected users is transmitted over the channel, producing an r-by-1 received vector $\mathbf{y}$ at the Node-B:

$$\mathbf{y} = \mathbf{H}\mathbf{G}_u\mathbf{P}_u^{1/2}\mathbf{s} + \mathbf{n}, \tag{1}$$

where $\mathbf{E}[\mathbf{s}\mathbf{s}^\dagger] = \mathbf{I}_u$, and $\mathbf{G}_u = \text{diag}\{G_1, G_2, \cdots, G_u\}$ denotes the path-loss matrix. The entries of the random matrix $\mathbf{H}$ are independent and identically distributed (i.i.d.) complex Gaussian distributed with zero mean and unit variance. The vector $\mathbf{n}$ is modeled as zero-mean additive white Gaussian noise (AWGN) with covariance matrix $\mathbf{E}[\mathbf{n}\mathbf{n}^\dagger] = \sigma_n^2\mathbf{I}_r$.

The power P_i allocated to user i is expected to convert into a certain data rate (more accurately a spectral efficiency), usually measured in terms of $\log_2(1+\gamma_i)$ with γ_i denoting the instantaneous signal-to-noise ratio (SNR) at the Node-B receiver for user i. We are interested in the energy-conversion efficiency, as defined by

$$EE_i = \frac{\log_2(1+\gamma_i)}{P_i + P_c} \text{ bps/Hz/Joule.} \tag{2}$$

The circuit power P_c is also included in the denominator for calculation; it represents the average energy consumed in the relevant electronic devices. Clearly, EE_i is a random variable, depending on the channel matrix $\mathbf{H}$. It is therefore more practical to consider its statistical average:

$$\eta_i(P_i) = \mathbf{E}_\mathbf{H}[EE_i] = \frac{E_\mathbf{H}[\log_2(1+\gamma_i)]}{P_i + P_c}, \tag{3}$$

which is sometimes called the achievable energy efficiency for i-th user, representing the ratio of the ergodic rate to the power consumption. For practical applications, the sum energy efficiency of all active users is more appealing, which is defined by [1]

$$\eta(u, \mathbf{P}_u) = \sum_{i=1}^{u} \eta_i = \sum_{i=1}^{u} \frac{E_\mathbf{H}[\log_2(1+\gamma_i)]}{P_i + P_c}. \tag{4}$$

Choosing an appropriate number of active users, i.e., $1 \leq u \leq r$, can be considered as choosing a *transmission mode* in the uplink V-MIMO system.

The value γ_i depends not only on the channel, but also on the post-processing technique to be used. In this paper, it is assumed that perfect CSI is available at the Node-B and the zero-forcing (ZF) detection method is employed at the receiver [16], leading to the decision variables

$$\mathbf{H}^\#\mathbf{y} = \text{diag}(P_1G_1, \cdots, P_uG_u)\mathbf{s} + \mathbf{H}^\#\mathbf{n}, \tag{5}$$

where $\mathbf{H}^\# = (\mathbf{H}^\dagger\mathbf{H})^{-1}\mathbf{H}^\dagger$ denotes the pseudo-inverse of $\mathbf{H}$. From (5), it follows that the output SNR for user i is given by

$$\gamma_i = \underbrace{(P_iG_i/\sigma_n^2)}_{\rho_i} \underbrace{\frac{1}{[(\mathbf{H}^\dagger\mathbf{H})^{-1})]_{ii}}}_{\xi_i}, \tag{6}$$

[1]Note that u in $\eta(u, \mathbf{P}_u)$ means that there are u users totally, while u in $\sum_{i=1}^{u} \eta_i$ means the u-th users in $\mathcal{B}'$

with $[\mathbf{A}]_{ii}$ signifying the i-th diagonal element of the matrix $\mathbf{A}$. For i.i.d. Rayleigh fading channels, $\mathbf{H}^{\dagger}\mathbf{H}$ follows the complex Wishart distribution as shown by $\mathbf{H}^{\dagger}\mathbf{H} \sim CW_u(r, \mathbf{I})$. Thus, the use of Theorem 3.2.11 of [15], [17] enables the assertion that ξ_i defined above is a chi-square variable with $2(r-u+1)$ degrees of freedom; i.e.,

$$\xi_i \sim \frac{1}{2}\chi^2(2(r-u+1)). \tag{7}$$

As such, we can represent the achievable energy efficiency for the i-th user as [18]

$$\eta_i(P_i) = \frac{E_{\xi_i}[\log_2(1+\rho_i\xi_i)]}{P_i + P_c}, \tag{8}$$

where $\rho_i = \frac{P_i G_i}{\sigma_n^2}$ is the received average SNR for user i. With the above notation, the sum energy efficiency of all active users in (4) can be rewritten as

$$\eta(u, \mathbf{P}_u) = \sum_{i=1}^{u} \frac{\mathbf{E}_{\xi_i}[\log_2(1+\rho_i\xi_i)]}{P_i + P_c}. \tag{9}$$

The maximization of the sum efficiency η in (9) requires efforts in two aspects. First, select an appropriate number of users, u, for transmission which corresponds to the selection of a transmission mode. Second, given a transmission mode, find an optimal power allocation strategy $\mathbf{P}_u$. Thus, the optimization at hand is to find u^* and $\mathbf{P}_u^*$ such that

$$\{u^*, \mathbf{P}_{u^*}^*\} = \arg\max_{u, \mathbf{P}_u} \ \eta(u, \mathbf{P}_u). \tag{10}$$

Clearly, this is a joint optimization problem.

III. Joint Mode Selection and Power Optimization Scheme

In the joint optimization defined in (10), the parameters to be optimized are interrelated. To optimize $\mathbf{P}_u$, we need to figure out u first; the same is true for optimizing the transmission mode u. To get rid of such an entanglement, we define a conditional objective function $\eta(\mathbf{P}_u|u)$ for a given number of active users u, and break the optimization problem (10) into two steps. In the first step, we find the conditional optimizers:

$$\mathbf{P}_u^* = \arg\max_{\mathbf{P}_u} \ \eta(\mathbf{P}_u|u), \tag{11}$$

for all $u = 1, 2 \ldots, r$. Then in the second step, the final solution is determined as

$$u^* = \arg \max_{v} \{\eta(P_v^*|v), \ v = 1, \ldots, r\}, \tag{12}$$

which defines the optimal power allocator $\mathbf{P}_{u^*}^*$. Clearly, (11) is the key step to our optimization problem. In what follows, we will address it under two possible operational conditions, i.e., without and with power constraint on transmission.

A. Optimization without power constraint

As indicated in (4), the ZF receiver decouples the interference among different users. Thus, without a power constraint, the maximization of the sum energy efficiency is equivalent to maximizing the energy efficiency of each active user as if it were operating in an interference-free environment. Nevertheless, the objective function η_i is highly nonlinear in P_i thereby raising a question as regard to the existence of the optimal solution and its uniqueness. The following assertions address this concern.

Proposition 1: There exists one and only one point $P_i^* \in (0, \infty)$ that maximizes $\eta_i(P_i)$. The function $\eta_i(P_i)$ is monotonic increasing over the interval $P_i \in (0, P_i^*]$ while monotonic decreasing over the interval $P_i \in (P_i^*, +\infty)$. However, regardless of its concavity over $P_i \in (0, P_i^*)$, $\eta_i(P_i)$ is neither concave nor convex over $P_i \in (P_i^*, \infty)$.

For a proof of these assertions, reader is referred to Appendix I-A for details.

Given the existence of the optimal power, it remains to determine it. To this end, we denote

$$f(\rho_i) = \mathbf{E}_{\xi_i}[\log_2(1+\rho_i\xi_i)], \ i = 1, \ldots, u, \tag{13}$$

so that the energy efficiency can be written as $\eta_i = f(\rho_i)/(P_i + P_c)$ where $\rho_i = P_i G_i/\sigma_n^2$. For a given number of active users, the optimal power P_i^* should satisfy the condition of $\frac{d\eta_i}{dP_i^*} = 0$, which, when simplified, reduces to

$$\alpha(P_i^*) \triangleq (G_i/\sigma_n^2)(P_i^* + P_c)f'(\rho_i^*) - f(\rho_i^*) = 0, \tag{14}$$

where $\alpha(P_i)$ is the numerator of $\frac{d\eta_i}{dP_i}$, which is defined in (48) of Appendix I-A. In addition, $\rho_i^* = P_i^* G_i/\sigma_n^2$ and the derivative of $f(\rho_i)$ with respect to ρ_i can be explicitly expressed by

$$f'(\rho_i) = \mathbf{E}_{\xi_i}\left[\frac{\xi_i}{(1+\rho_i\xi_i)\ln 2}\right]. \tag{15}$$

The optimal power is a root of the nonlinear function $\alpha(P_i)$ defined above, to which a closed-form solution to (13) is difficult to find. A numerical solution can be obtained by resorting to the Newton-Raphson iteration method. Specifically, the $(k+1)$-th iteration of the optimal power is related to the k-th one by

$$P_i^*(k+1) = P_i^*(k) - \frac{\alpha(P_i^*(k))}{\alpha'(P_i^*(k))}, \tag{16}$$

where $\alpha'(P_i)$ is the first-order derivative of $\alpha(P_i)$ with respect to P_i, and can be shown as

$$\alpha'(P_i) = (G_i/\sigma_n^2)^2 f''(\rho_i)(P_i + P_c), \tag{17}$$

with $f''(\rho_i)$ denoting the second-order derivative of $f(\rho_i)$ with respect to ρ_i. To ensure the fast convergence of the solution, we specified the initialization of $P_i^*(1) = 0$. Further, we check $P_i^*(k)$ at every iteration. In case of $P_i^*(k) < 0$, we will set $P_i^*(k+1)$ a small positive value ϵ to restart the iterative process. In the same manner, we calculate P_i^* for all $1 \le i \le u$, obtaining the optimal power vector $\mathbf{P}_u^* = [P_1^*, \ldots, P_u^*]$ for a given transmission mode.

B. Optimization with power constraint

Many practical communication systems are usually subject to a constraint on their total power consumption $\sum_{i=1}^{u}(P_i + P_c)$, such that

$$P_{\min} \le (uP_c + \underbrace{P_1 + \cdots + P_u}_{P^+}) \le P_{\max} \tag{18}$$

where the lower bound $P_{\min}$ is set to ensure the necessary data rate whereas the upper bound $P_{\max}$ is set to meet the peak power limit. The physical implication of $P_{\min}$ is relatively less explicit than $P_{\max}$, due to the fact that the data rate also depends on the channel gains of active users. Nevertheless, its inclusion in the optimization is well justified from two aspects. First, the case without a lower bound constraint can be easily implemented by setting $P_{\min} = 0$. Second, the power efficiency is a non-convex function which, without a lower power constraint $P_{\min}$, is likely to maximize at a very transmit power. The consequence is the failure to meet the minimum data rate requirement. According to our practice, it suffices to choose $P_{\min}$, in conjunction with the median channel gain, to meet the data rate requirement. Further denoting

$$\begin{aligned} P'_{\min} &= P_{\min} - uP_c \\ P'_{\max} &= P_{\max} - uP_c, \end{aligned} \tag{19}$$

we can rewrite the power constraint in (18) as

$$P'_{\min} \le P^+ \le P'_{\max} \tag{20}$$

whereby the optimization problem is expressible as

$$\begin{aligned} (\mathbf{P1}) \qquad & \max_{\mathbf{P}_u} \ \eta(u, \mathbf{P}_u) \\ & s.t.\ P'_{\min} \le P^+ \le P'_{\max} \end{aligned} \tag{21}$$

Imposing a power constraint will alter the optimization interval and thus, the optimization strategy. The changes very depend on the values of $P_{\max}$ and $P_{\min}$ relative to the unconditioned optimizer $\mathbf{P}^*$. We can identify three different cases, which require different techniques to handle. Hereafter, we will use $sum(\mathbf{P})$ to denote the sum of all the entries in vector $\mathbf{P}$ for notational simplicity.

1) Case 1: $P'_{\min} \le$ sum$(\mathbf{P}^*_u) \le P'_{\max}$: In this case, the global solution falls in to the feasible region. Accordingly, the unconstrained optimal solution $\mathbf{P}^*_u$ is also the solution to the constrained one described in $(\mathbf{P1})$.

2) Case 2: sum$(\mathbf{P}^*_u) > P'_{\max}$: Let $\mathbf{P}^{**}_u = [P^{**}_1, P^{**}_2, \cdots, P^{**}_u]$ denote the optimal solution to the Problem $(\mathbf{P1})$. Given the constraint sum$(\mathbf{P}^*_u) > P'_{\max}$, we can use the method of contradiction alongside Proposition 1 to show that

$$P^{**}_i \le P^*_i, \ \forall i \in \{1, 2, \cdots, u\}. \tag{22}$$

A detailed proof is given in Appendix I-B. This result simply indicates that the optimal value P^{**}_i for each constituent user is located in the concave region of $\eta_i(P_i)$, in accordance with Proposition 1. We can thus assert that the entire optimal power vector $\mathbf{P}^{**}_u$ is located in the concave region of $\eta(u, \mathbf{P}_u)$. Therefore, the local optimum is also the global optimum for the problem $(\mathbf{P1})$.

With the optimizer located inside the concave interval, the use of the Karush-Kuhn-Tucker(KKT) conditions enables us to re-state the optimization problem $(\mathbf{P1})$ as follows.

Proposition 2: When $sum(\mathbf{P}^*_u) > P'_{\max}$, the optimization problem $(\mathbf{P1})$ is equivalent to the one stated below.

$$\begin{aligned} (\mathbf{P2}) \qquad & \max_{\mathbf{P}_u} \ \eta(u, \mathbf{P}_u) \\ & s.t. \sum_{i=1}^{u} P_i = P'_{\max} \end{aligned}$$

For a proof, see Appendix I-C. This new formulation allows us to employ the gradient projection (GP) method to search for its optimal solution [21], as outlined below where $\mathcal{S} = \{\mathbf{P}_u | \sum_{i=1}^{u} P_i = P'_{\max}\}$.

GP algorithms :

Step 0: Calculate the projection matrix $\Omega = \mathbf{I} - \mathbf{a}(\mathbf{a}^T\mathbf{a})^{-1}\mathbf{a}^T$, where $\mathbf{a}^T = [1, 1, \cdots, 1]$.

Step 1: Calculate the gradient vector $\nabla\eta(\mathbf{P}_u) = [\frac{\partial\eta}{\partial P_1}, \frac{\partial\eta}{\partial P_2}, \cdots, \frac{\partial\eta}{\partial P_u}]^T$.

Step 2 : Calculate the vector $\mathbf{d} = \Omega\nabla\eta(\mathbf{P}_u)$.

Step 3 : If $\|\mathbf{d}\| \le \varepsilon$, terminate.

Step 4 : Determine the maximum step size $\alpha_{\max} = \arg\max_{\alpha}(\mathbf{P}_u + \alpha\mathbf{d} \in \mathcal{S})$, and solve the linear-search problem $\max \eta(u, \mathbf{P}_u + \alpha\mathbf{d})$ for $0 \le \alpha \le \alpha_{\max}$.

Step 5 : Set $\mathbf{P}_u = \mathbf{P}_u + \alpha\mathbf{d}$, and go to Step 1.

3) Case 3: sum$(\mathbf{P}^*_u) < P'_{min}$: For this case, let $\mathbf{P}^{***}_u = (P^{***}_1, P^{***}_2, \cdots, P^{***}_u)$ as the solution to the Problem $(\mathbf{P1})$. Following the same token as to derive (22), we can make the following assertion:

$$P^{***}_i \ge P^*_i, \ \forall i \in \{1, 2, \cdots, u\}. \tag{23}$$

From Proposition 1, η_i is non-concave over the region $(P^*_i, +\infty)$, thus making the optimization problem at hand extremely difficult to handle.

In this paper, since the number of constituent users is limited in uplink, we solve such an optimization problem by using, instead, the simulated annealing (SA) algorithm. The SA algorithm is a probabilistic method developed by Kirkpatrick [22] and Cerny [23] for finding the global optimum of a cost function which might have several local optima.

C. Mode selection for energy efficiency

In the previous analysis, we showed how to determine the optimal transmission mode and the corresponding power allocator for for both the cases with and without a power constraint. The optimizers so obtained clearly depend on the channel conditions including SNR, average channel propagation loss, and the power constraint setting $P_{\min}$ and $P_{\max}$. Thus, as the channel conditions change, the transmission mode needs to adapt itself to the changing operational environment. This can be done by efficient techniques derived in the preceding subsections, and the global method with an exhaustive search over all possible user combinations can be directly employed. To further reduce the computational complexity, a suboptimal solution for mode selection will be described in the next section.

IV. Mode Pre-selection for Complexity Reduction

In the preceding section, the optimization of the energy efficiency was done by comparing the conditional power optimizers exhaustedly for all the possible transmission modes $1 \le u \le r$. This type of exhausted enumeration is time consuming.

The computational complexity will be considerably reduced if we can narrow down the range for u, from some theoretical perspective, before power optimization. Though suboptimal in nature, the result so obtained is very close to the global optimal solution, as will be demonstrated in Section V.

Since we want to determine the most likely transmission modes without performing power allocation, it is reasonable to assume that each user transmits its signal with the maximal power. In this paper, we assume all users have the same maximal power, denoted as P. With these conditions, (9) can be rewritten as:

$$\eta(u) = \sum_{i=1}^{u} \frac{\mathbf{E}_{\xi_i}[\log_2(1+\rho_i\xi_i)]}{P+P_c} \tag{24}$$

where $\rho_i = G_iP/\sigma_n^2$. Note that the denominator is now of irrelevance to the transmission mode. Thus, by denoting

$$\mathcal{R}(u) = \sum_{i=1}^{u} \underbrace{\mathbf{E}_{\xi_i}[\log_2(1+\rho_i\xi_i)]}_{R_i(k)} \tag{25}$$

where $k = r-u+1$ denotes the diversity order by each user. The maximization of η reduces to the maximization of $\mathcal{R}$, namely, to find the optimal transmission mode u^* for which,

$$u^* = \arg\max_{1\le u\le r} \mathcal{R}(u). \tag{26}$$

Physically, $\mathcal{R}(u)$ is the sum ergodic rate of all u users and correspondingly, $R_i(u)$ is the ergodic rate of the i-th user in (25). Recall that transmission rate, up to a normalization factor, represents the spectral efficiency. The expression (26) suggests that the selection of optimal transmission mode can be done on the basis of spectral efficiency maximization, at least at the level of a suboptimal solution.

First, we investigate the behavior of each component in $\mathcal{R}$, ending up with results described below.

Proposition 3: Denote the ergodic rate of one user with channel gain G as $R(k) = \mathbf{E}_\xi[\log_2(1+\rho\xi)]$ where $\xi \sim \chi^2(2k)$, $k = r-u+1$, and $\rho = \frac{PG}{\sigma^2}$. Then $R(k)$ increases monotonically with k, and is concave with k, i.e.,

$$\Delta_R^1(k) = R(k+1) - R(k) > 0, \tag{27}$$

$$\Delta_R^2(k) = \Delta_R^1(k+1) - \Delta_R^1(k) < 0. \tag{28}$$

Proof: To show the monotone increasing property, by definition we can write the first-order difference as

$$\begin{aligned}\Delta_R^1(k) &= R(k+1) - R(k)\\ &= \frac{\log_2(e)}{k!}\int_0^\infty \ln(1+\rho x)x^k e^{-x}dx -\\ &\frac{\log_2(e)}{(k-1)!}\int_0^\infty \ln(1+\rho x)x^{k-1}e^{-x}dx,\end{aligned} \tag{29}$$

where the second integral is expressible in a similar form as $R(k+1)$ via integration by part to yield

$$\begin{aligned}&\int_0^\infty \ln(1+\rho x)x^{k-1}e^{-x}dx\\ &= \frac{1}{k}[\ln(1+\rho\,x)e^{-x}x^k|_0^\infty - \int_0^\infty (\ln(1+\rho\,x)e^{-x})'x^k dx]\\ &= \frac{1}{k}\int_0^\infty [\ln(1+\rho\,x) - \frac{\rho}{1+\rho x}]e^{-x}x^k dx,\end{aligned} \tag{30}$$

where the part outside the integral will be zero, since

$$\begin{aligned}&\ln(1+\rho\,x)e^{-x}x^k|_0^\infty\\ &= \lim_{x\to\infty}\ln(1+\rho\,x)e^{-x}x^k - \lim_{x\to 0}\ln(1+\rho\,x)e^{-x}x^k\\ &= 0-0=0.\end{aligned} \tag{31}$$

Inserting (30) into (29) leads to

$$\Delta_R^1(k) = \frac{\log_2(e)}{k!}\int_0^\infty \frac{\rho}{1+\rho x}e^{-x}x^k dx > 0. \tag{32}$$

By the same token, we proceed for the second-order difference yielding

$$\begin{aligned}\Delta_R^2(k) &= \Delta_R^1(k+1) - \Delta_R^1(k)\\ &= -\frac{\log_2(e)}{(k+1)!}\int_0^\infty \frac{\rho^2}{(1+\rho x)^2}e^{-x}x^{k+1}dx < 0\end{aligned} \tag{33}$$

which along with (32) completes the proof.

The use of Proposition 3 to (25), alongside the fact that $k = r-u+1$, enables us to assert that each $\mathcal{R}_i$ decreases with the number of active users u. Clearly, as the summation of u terms, $\mathcal{R}$ increases with u on one hand whereas each summand decreases with u on the other. As such, there must be an optimal transmission mode u^* that maximizes the sum energy efficiency.

A few remarks are made here. Note that R_i depends on the channel gain G_i through $\rho_i = \frac{PG_i}{\sigma^2}$. Thus, how to select u^* active users among all U users is a key issue for the optimization problem (25). In general, a better performance can be obtained if we select those users who are nearer to the BS to ensure larger channel gains. However, from the whole system point of view, we should consider the fair issue, which means that every user should have a chance to transmit. If we select users solely based on the energy efficiency performance, we cannot guarantee the transmission chance of users far away from the BS. On the contrary, if we select users randomly, every user is equal to each other, certainly at the cost of performance decay. There is a tradeoff between the performance and the fair issue. In this paper, we aim to guarantee fair transmission and select users randomly.

We next consider an important special case of isometric networks, for which (25) can be simplified. The term isometric network implies identical propagation loss for all users, i.e., $G_i = G$ (for $1 \le i \le U$) which, in turn, implies equal SNR ρ_i and equal rate $R_i(k)$ for all the users, i.e., $\rho_i = \rho = \frac{PG}{\sigma^2}$ and $R_i(k) = R(k)$. Thus, we can rewrite (25) as

$$\mathcal{R}(u) = uR_i(r-u+1) \tag{34}$$

which, by changing the variable $u = r-k+1$, is alternatively expressible as

$$\mathcal{R}(k) = (r-k+1)R(k) \tag{35}$$

with $R(k)$ defined in Proposition 3.

Lemma 1: The sum rate $\mathcal{R}(k)$ is a concave function of the diversity order k for each user.

Proof: By direct calculation, it is easy to obtain

$$\begin{aligned}\Delta_{\mathcal{R}}^1(k) &= \mathcal{R}(k+1) - \mathcal{R}(k)\\ &= (r-k+1)\Delta_R^1(k) - R(k+1)\end{aligned} \tag{36}$$

whereby the second-order difference can be determined as

$$\begin{aligned}&\Delta_{\mathcal{R}}^2(k) = \Delta_{\mathcal{R}}^1(k+1) - \Delta_{\mathcal{R}}^1(k)\\ &= [(r-k)\Delta_R^1(k+1) - R(k+2)] -\\ &[(r-k+1)\Delta_R^1(k) - R(k+1)]\\ &= (r-k+1)\Delta_R^2(k) - 2\Delta_R^1(k+1).\end{aligned} \tag{37}$$

TABLE I
SIMULATION PARAMETERS

Frame duration	0.5 ms
N_t (# of Tx antenna at user)	1
r (# of Rx antenna at Node-B)	2 or 4
u (# of paired user)	1-2 or 1-4
U (# of users per sector)	20
Carrier frequency	2 GHz
Sampling frequency	7.68 MHz
Pairing update	Per frame
Receiver	Zero forcing
Channel estimation	Perfect
Traffic model	Full buffer
# of frames	5000
Circuit power P_c	0.2

Now, from Proposition 3, we know that $\Delta_R^2(k) < 0$ and $\Delta_R^1(k+1) > 0$. We can thus assert $\Delta_{\mathcal{R}}^2(k) < 0$ which completes the proof.

By virtue of Lemma 1, we are in position to present a main result for isometric networks.

Proposition 4: Asymptotically, the optimal transmission mode for Asymptotically, the optimal transmission mode for isometric networks is given by

$$u^* = \begin{cases} [\frac{r}{2}+1] & \rho \to 0 \\ r & \rho \to \infty. \end{cases} \tag{38}$$

where $[x]$ denotes the integer part of x.

Proof: In (36), using the rule of integration by part leads to

$$\begin{aligned} &\Delta_{\mathcal{R}}^1(k) = (r-k+1)\Delta_R^1(k) - R(k+1) \\ &= (r-k+1)\frac{\log_2(e)}{k!}\int_0^\infty \frac{\rho}{1+\rho x}e^{-x}x^k dx - \\ &\frac{\log_2(e)}{k!}\int_0^\infty \ln(1+\rho x)x^k e^{-x}dx \\ &= (r-k)\frac{\log_2(e)}{k!}\int_0^\infty \frac{\rho}{1+\rho\, x}e^{-x}x^k dx - \\ &k\frac{\log_2(e)}{k!}\int_0^\infty \ln(1+\rho x)x^{k-1}e^{-x}dx \end{aligned} \tag{39}$$

which, by passing $\rho \to 0^+$, yields

$$\begin{aligned} &\Delta_{\mathcal{R}}^1(k) \approx (r-k)\frac{\log_2(e)}{k!}\int_0^\infty \rho e^{-x}x^k dx - \\ &k\frac{\log_2(e)}{k!}\int_0^\infty \rho x x^{k-1}e^{-x}dx \\ &= \frac{\log_2(e)}{k!}\rho(r-2k)\int_0^\infty e^{-x}x^k dx. \end{aligned} \tag{40}$$

From the last line, we can investigate the item of $r-2k$. If $k \le [\frac{r}{2}]$, then $\Delta_{\mathcal{R}}^1(k) \to 0^+$. On the other hand, if $k \ge [\frac{r}{2}+1]$, then $\Delta_{\mathcal{R}}^1(k) \to 0^-$. Therefore, it follows that $\Delta_{\mathcal{R}}^1([\frac{r}{2}]) \ge 0$ and $\Delta_{\mathcal{R}}^1([\frac{r}{2}+1]) < 0$. Hence, we have $k^* = [\frac{r}{2}]$ leading to $u^* = r - k^* + 1 = [\frac{r}{2}+1]$.

Algorithm 1 Low-Complexity Pre-Selection Algorithm

Initialize:
  Denote $u^* = 0$ as optimal transmission mode.
  Denote $\eta^* = 0$ as maximal energy efficiency.
for $[\frac{r}{2}+1] \le u \le r$ **do**
  Doing optimal power allocation and obtain the maximal EE $\eta(u)$ according to (11) in Sec-III.
  if $\eta(u) > \eta^*$ **then**
    $\eta^* = \eta(u)$.
    $u^* = u$.
  end if
end for

Next, letting $\rho \to \infty$, we obtain

$$\begin{aligned} &\Delta_{\mathcal{R}}^1(1) = r\Delta_R^1(1) - R(2) \\ &= \log_2(e)\int_0^\infty [\frac{r\rho}{1+\rho x} - \ln(1+\rho x)]xe^{-x}dx < 0 \\ &(\text{Since } \frac{r\rho}{1+\rho x} - \ln(1+\rho x) < 0 \text{ when } \rho \to \infty). \end{aligned} \tag{41}$$

From Lemma 1, $\mathcal{R}(k)$ is a concave function of k, i.e., $\Delta_{\mathcal{R}}^1(k)$ is decreasing with k. Hence, (41) follows that $\Delta_{\mathcal{R}}^1(k) < 0$ and $k^* = 1$, which leads to $u^* = r$.

Another main result for isometric networks is summarized as follows.

Proposition 5: For a general SNR ρ, the optimal transmission mode of isometric networks can be narrowed down, ranging between $[\frac{r}{2}+1]$ and r; namely,

$$[\frac{r}{2}+1] \le u^* \le r. \tag{42}$$

Proof: When $k = [\frac{r}{2}]$, we have

$$\begin{aligned} &\Delta_{\mathcal{R}}^1(k) = r\Delta_R^1(k) - R(k+1) \\ &= (r-k)\frac{\log_2(e)}{k!}\int_0^\infty \frac{\rho}{1+\rho x}e^{-x}x^k dx \\ &-k\frac{\log_2(e)}{k!}\int_0^\infty \ln(1+\rho x)x^{k-1}e^{-x}dx \\ &= \frac{r}{2}\frac{\log_2(e)}{k!}\int_0^\infty [\frac{\rho x}{1+\rho x} - \ln(1+\rho x)]e^{-x}x^{k-1}dx \\ &< 0 \ (\text{Since } \frac{\rho x}{1+\rho x} - \ln(1+\rho x) < 0). \end{aligned} \tag{43}$$

Thus $k^* \le [\frac{r}{2}]$ and $u^* \ge [\frac{r}{2}+1]$ which, when combined, allow us to write $[\frac{r}{2}+1] \le u^* \le r$.

Based on the theory derived in this section, a low complexity pre-selection technique for transmission mode has been developed, which is summarized in Algorithm 1 for ease of use.

V. SIMULATION RESULTS

In this section, we examine the energy efficiency of the proposed mode-switching scheme with optimal power allocation for uplink V-MIMO systems. For simplicity, we assume a single cell scenario in which each user is assigned with all resource blocks, and the Node-B employs a ZF receiver with perfect CSI and perfect synchronization. The detailed simulation parameters are listed in Table I.

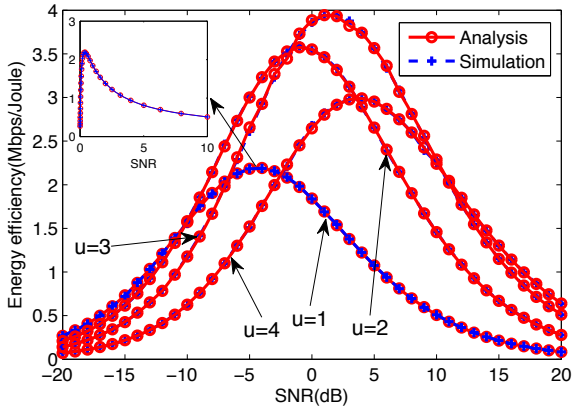

Fig. 1. Behaviors of energy efficiency as a function of SNR and user number u with $r = 4$.

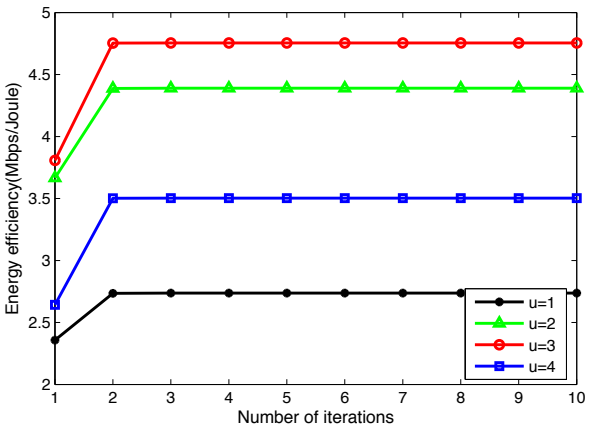

Fig. 2. Convergence to the maximum energy efficiency with iterations.

We first investigate the behavior of the energy efficiency (i.e., the objective) function defined in (9) by setting $r = 4$ and $P_i = P/u$ for all $i = 1, 2, \cdots, u$ with SNR$= \frac{P}{\sigma_n^2}$ in Fig. 1. It is observed that an optimal transmission mode (i.e., the optimal number of active users) does exist over a certain range of SNRs. For example, $u = 1$ outperforms other modes over SNR$\in (-20, -10)$dB, and so does u over SNR$\in (-10, -2)$dB. If we plot the curves in the linear scale as shown in the small window for $u = 1$, it is also observed that there exists a unique peak in the energy efficiency curve. The objective function is concave before the peak value and becomes neither concave nor convex, as asserted in Proposition 1. The curves based on simulations are also included for comparison. In addition, regarding the impact of ZF receiver at low SNR region, we know only single user transmission mode will be the optimal from our analysis and simulation. Then, determining the SU transmission mode, we can also perform the more optimal receivers to further improve the performance at the BS.

The existence of a unique optimal transmission mode lays a foundation for its numerical search based on, for instance, the Newton-Raphson method. The convergence behavior of energy efficiency with iterations is illustrated in Fig. 2 where the parameters are set to $r = 4$. Clearly, the EE rapidly converges to its optimum, shortly in 2 steps.

For an isometric network with a total power constraint between $P_{\min}$ and $P_{\max}$, based on the result in Section III, each optimal transmission mode can be determined for a given scenario. Accordingly, the operating regions for different modes can be plotted for different system parameters. Fig. 3(a) shows the operating regions for the system with different power constraint, for X-axis $P_{\min}$ and Y-axis $P_{\max}$, respectively, where each mark on the figure denotes the type of the active mode. The influence of $\delta_p = P_{\max} - P_{\min}$ on the achievable energy efficiency is shown in Fig. 3(b). When δ_p is small, single user (SU) mode $u = 1$ is first activated, and then switch to other modes as the operating conditions change. Increasing δ_p from 1 dB to 5dB broadens the range of attaining the highest achievable EE.

Let us consider a heterogeneous network with two receive antennas (i.e., $r = 2$), maximum of $u = 2$ users, unequal path

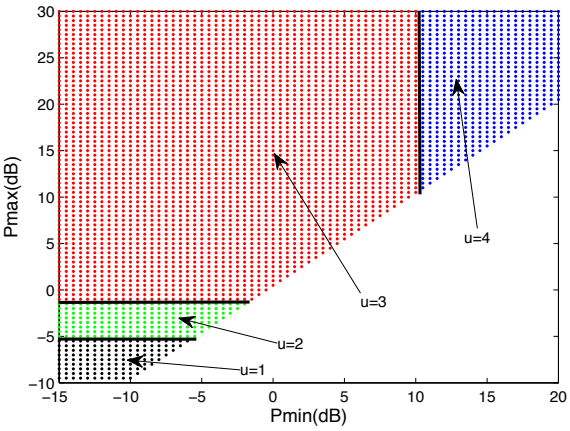

(a) Operating regions.

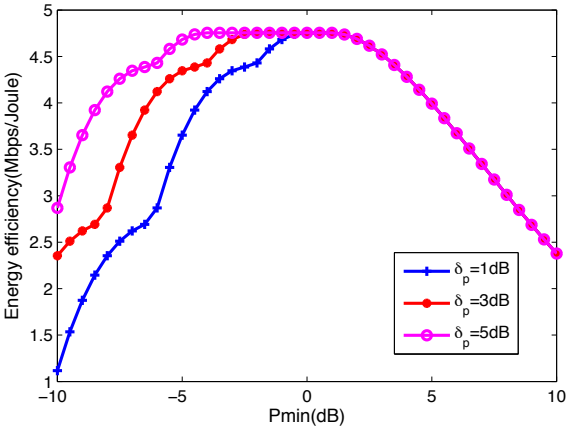

(b) Variation of energy efficiency with different $\delta_p = P_{\max} - P_{\min}$.

Fig. 3. Operating regions and energy efficiency in the isometric network with $r = 4$.

loss $G_1 = 4$ and $G_2 = 1$, and subject to a power constraint defined by a two-tuple $(P_{\min}, \delta_p)$. We first investigate the effect of optimal power allocation *alone* for a fixed number of users $u = 2$, with results plotted in Fig. 4. When $P_{\min}$ moves along the horizontal axis, each curve experiences a power-constraint moving window of fixed width δ_p. The changing

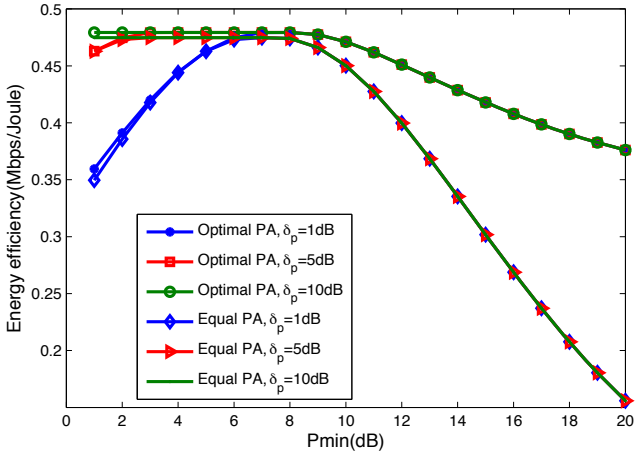

Fig. 4. Optimal power vs. equal power allocation in a heterogeneous network with $r = 2$ and different $\delta_p = P_{\max} - P_{\min}$.

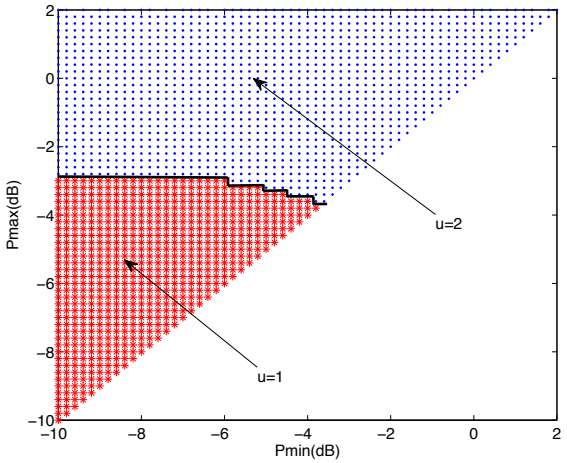

(a) Operating regions.

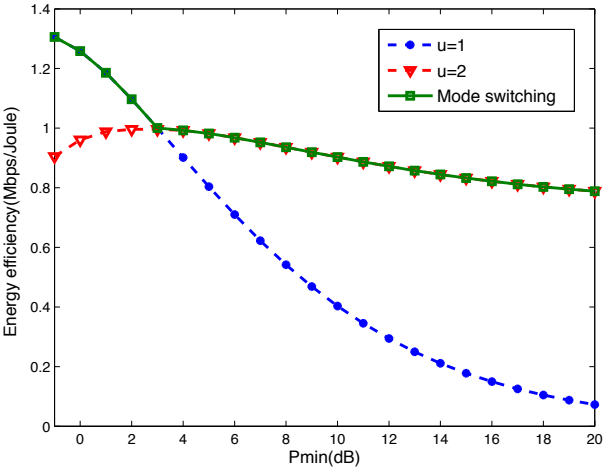

(b) Energy efficiency for joint mode switching and optimal power allocation.

Fig. 5. Operating regions and energy efficiency comparisons in a heterogeneous network with $r = 2$.

power-constraint window alters the position of the constrained optimal power maximizer relative to the global optimal one, and thus requires re-evaluating the optimal power allocation by virtue of the techniques developed in Section III.B. The curves so obtained are labeled with "Optimal PA." Results without power optimization are also included for comparison, which correspond to equal power allocation and are thus labeled with "Equal PA." The curves for "Equal PA" are obtained by assigning equal power to all users and searching over the total power constraint range for a maximal EE output. As expected, the EE with optimal power allocation much exceeds its equal PA counterpart over a wide range, especially for large $P_{\min}$ and large δ_p. The reason is that under these condition, the constrained optimal power allocator attains or is closer to the global optimal one.

Under the same heterogeneous network setting, we perform joint optimization for both transmission mode and power allocation. The optimal transmission mode so obtained is certainly a function of $P_{\min}$ and $P_{\max}$. The distribution of the optimal transmission mode over the $P_{\min} - P_{\max}$ plane is depicted in Fig. 5(a) with each zone in the upper half-plane $P_{\max} > P_{\min}$ corresponding to an optimal u. Thus, for a given pair of $(P_{\min}, P_{\max})$, we can identify the corresponding zone whereby the optimal transmission mode is determined. Fig. 5(b) heuristically shows mode switching between $u = 1$ and $u = 2$ for the case of $\delta_p = 5$dB.

Return to isometric networks. If transmission mode optimization is done with the maximum power constraint on each user instead, the optimal mode distribution reduces to one dimension, simply depending on the SNR, as shown in Fig. 6. In Section VI, we assert that the optimal transmission mode is located between $[\frac{r}{2} + 1] \leq u^* \leq r$; this is exactly the case as indicated in the figure. We also observe that the optimal transmission mode approaches $u^* = [\frac{r}{2} + 1]$ for low SNR, whereas tends to $u^* = r$ for high SNR, agreeing with our theoretic analysis.

Next consider the application of the low-complexity transmission mode pre-selection (LCPS) technique to isometric networks, with results graphed in Fig. 7. The results obtained by the global optimization algorithm (GO) is also included as a bench mark for comparison. For most power constraint situations, the LCPS performs equally well as the GO. The gap appears in the low $P_{\min}$ region; the reason is that the transmission modes with larger u are not feasible. However, the gap will be reduced as δ_p increases, as shown in this figure. Therefore in overall, the LCPS algorithm is an effective technique. Finally, the impact of r upon EE in the LCPS system is illustrated in Fig. 8 where $\delta_p = 3$dB. We can see that in the low $P_{\min}$ region, a larger r leads to a larger gap between the GO and LCPS . This can be explained just like in Fig. 7. Due to the sum circuit power consumption, a larger r will make more transmission modes infeasible in low $P_{\min}$. Particularly, when $r = 12$ and $P_{\min} \leq -4.5$dB, all transmission modes with $r > 6$ are infeasible, which leads to zero EE with LCPS algorithm as shown in the figure.

VI. Conclusion

In this paper, we propose a joint mode selection and power loading scheme that adaptively selects active transmission

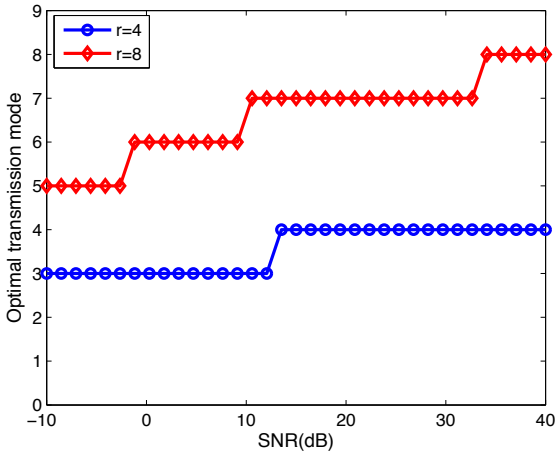

Fig. 6. Optimal transmission mode with different SNR.

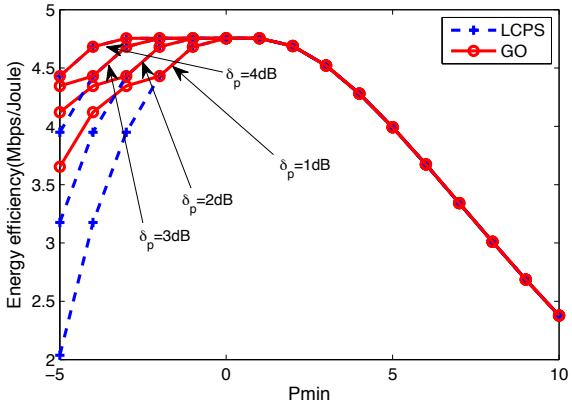

Fig. 7. Energy efficiency comparison between GO and LCPS algorithms with different $\delta_p = P_{\max} - P_{\min}$.

mode based on the achievable energy efficiency in uplink V-MIMO systems. Joint transmit and circuit power consumptions are taken into account to dramatically improve energy efficiency for different transmission modes. We first obtain the achievable EE expressions for different transmission modes based on the ergodic rates together with transmission and circuit power. Then we analyze the properties of the achievable EE with the transmission mode, which demonstrate the existence of a unique globally optimal solution to maximize energy efficiency for different transmission modes without power constraint. Furthermore, when considering the sum power constraint, the optimal power allocation for each transmission mode is exploited with three cases. After obtaining the optimal EE for each transmission mode, it is readily to get the optimal transmission mode in different power constraints. Furthermore, to reduce the computation complexity, a suboptimal algorithm in term of mode pre-selection is proposed. Finally, the simulation results substantiate the effectiveness of our proposed joint mode switching and power loading scheme. The idea in this paper could be applied to cognitive networks [24] or large scale wireless networks [25] etc.

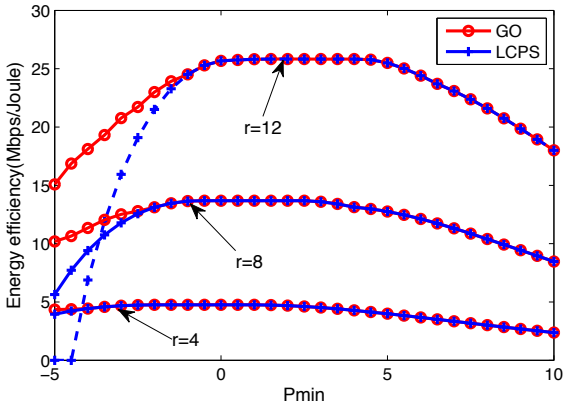

Fig. 8. Energy efficiency comparison between GO and LCPS algorithms with different r.

ACKNOWLEDGEMENT

This work was supported by National High Technology Research and Development Program (863 Program) of China under Grant No. 2011AA01A105, Key Deployment Project of Chinese Academic of Sciences (KGZD-EW-103), Fund of Youth Innovation Promotion Association of Chinese Academy of Sciences, and Open Research Fund of the State Key Laboratory of Integrated Services Networks, Xidian University, China. The work of Q. T. Zhang was supported by the Research Grants Council, Hong Kong Special Administrative Region, China under Project CityU 124911. The work of Peng Cheng was supported by the fund of Innovation Project of Shanghai Jiao Tong University under Grant No. AE0300063.

APPENDIX A

A. Proof of Proposition 1

We denote $f(\rho_i) = \mathbf{E}_{\xi_i}[\log_2(1+\rho_i\xi_i)]$. Then we have $\eta_i(P_i) = \frac{f(\rho_i)}{P_i+P_c}$ where $\rho_i = \frac{P_i G_i}{\sigma^2}$ and $\xi_i \sim \frac{1}{2}\chi^2(2k)$.

Since

$$f(\rho_i) = \int_0^\infty \log_2(1+\rho_i x)\frac{1}{(k-1)!}x^{k-1}e^{-x}dx, \quad (44)$$

then

$$f'(\rho_i) = \frac{\partial f(\rho_i)}{\partial \rho_i} = \frac{\log_2(e)}{(k-1)!}\int_0^\infty \frac{1}{1+\rho_i x}x^k e^{-x}dx, \quad (45)$$

and

$$f''(\rho_i) = \frac{\partial^2 f(\rho_i)}{\partial \rho_i^2} = -\frac{\log_2(e)}{(k-1)!}\int_0^\infty \frac{1}{(1+\rho_i x)^2}x^{k+1}e^{-x}dx. \quad (46)$$

Next we can get the first derivative of $\eta_i(P_i)$ with P_i, that is

$$\frac{\partial \eta_i(P_i)}{\partial P_i} = \frac{G_i/\sigma^2 f'(\rho_i)(P_i+P_c) - f(\rho_i)}{(P_i+P_c)^2}. \quad (47)$$

For the numerator part, we define

$$\alpha(P_i) = G_i/\sigma^2 f'(\rho_i)(P_i+P_c) - f(\rho_i). \quad (48)$$

Then, from (46), we know that $f''(\rho_i) < 0$, thus

$$\alpha'(P_i) = (G_i/\sigma^2)^2 f''(\rho_i)(P_i + P_c) < 0. \quad (49)$$

Thus, $\alpha(P_i)$ is a decreasing function with P_i. Furthermore,

$$\lim_{P_i \to 0} \alpha(P_i) = \lim_{P_i \to 0} G_i/\sigma^2 f'(\rho_i)(P_i + P_c) - f(\rho_i)$$
$$= \lim_{P_i \to 0} P_c G_i/\sigma^2 f'(\rho_i) - f(\rho_i). \quad (50)$$

Indeed, $\lim_{P_i \to 0} f(\rho_i) = 0$, then,

$$\lim_{P_i \to 0} \alpha(P_i) = \lim_{P_i \to 0} P_c G_i/\sigma^2 f'(\rho_i) > 0. \quad (51)$$

On the other hand,

$$\lim_{P_i \to \infty} \alpha(P_i) = \lim_{P_i \to \infty} G_i/\sigma^2 f'(\rho_i)(P_i + P_c) - f(\rho_i)$$
$$= \lim_{P_i \to \infty} \frac{G_i/\sigma^2 f'(\rho_i)(P_i + P_c) - f(\rho_i)}{P_i} P_i$$
$$= \lim_{P_i \to \infty} \frac{d(G_i/\sigma^2 f'(\rho_i)(P_i + P_c) - f(\rho_i))/dP_i}{d(P_i)/dP_i} P_i$$
$$= \lim_{P_i \to \infty} (G_i/\sigma^2)^2 f''(\rho_i)(P_i + P_c) P_i < 0. \quad (52)$$

As a result, from (49)-(52), we can deduce that $\alpha(P_i)$ is first larger than 0, then decreasing to less than zero. Since the denominate item in (48) is always larger than 0, there exists the unique P_i^* for $\frac{\partial \eta_i(P_i^*)}{\partial P_i^*} = 0$. Moreover, for $P_i < P_i^*$, $\eta_i(P_i)$ is increasing as $\frac{\partial \eta_i(P_i)}{\partial P_i} > 0$, and for $P_i > P_i^*$, $\eta_i(P_i)$ is decreasing as $\frac{\partial \eta_i(P_i)}{\partial P_i} < 0$. Thus, P_i^* will be the unique point which is a global maximizer of η_i, i.e., $P_i^* = \arg\max_{P_i \in [0, +\infty)} \eta_i(P_i)$.

At the same time, we can get the second derivative of $\eta_i(P_i)$ with P_i, i.e.,

$$\frac{\partial^2 \eta_i(P_i)}{\partial P_i^2} = \frac{\alpha'(P_i)(P_i + P_c)^3 - 2\alpha(P_i)(P_i + P_c)}{(P_i + P_c)^4}. \quad (53)$$

Since $\alpha'(P_i) < 0$ and $\alpha(P_i) > 0$ at the interval $P_i \in (0, P_i^*]$, we can obtain $\frac{\partial^2 \eta_i(P_i)}{\partial P_i^2} < 0$, which means $\eta_i(P_i)$ is concave. While for the interval $P_i \in (P_i^*, +\infty)$, $\frac{\partial^2 \eta_i(P_i)}{\partial P_i^2}$ can be either positive or negative, thus $\eta_i(P_i)$ is neither concave nor convex. In conclusion, $\eta_i(P_i)$ is concave at the interval $P_i \in (0, P_i^*)$, but neither concave nor convex at the interval $P_i \in [P_i^*, +\infty)$.

B. Proof of (22) and (23)

We will prove by contradiction. Assume $\exists i \in \{1, 2, \cdots, u\}$, $P_i^{**} > P_i^*$ when $\sum_{i=1}^u P_i^* > P'_{\max}$. Since $\mathbf{P}_u^{**}$ is the solution to the Problem $(\mathbf{P1})$, $\mathbf{P}_u^{**}$ will satisfy the constraint of Problem $(\mathbf{P1})$, i.e., $P'_{\min} \le \sum_{j=1}^u P_j^{**} \le P'_{\max}$. Then $\exists k \in \{1, 2, \cdots, u\}$ and $k \neq i$, $P_k^{**} < P_k^*$(otherwise, if $P_k^{**} \ge P_k^*$ for all $k \neq i$, we have $\sum_{j=1}^u P_j^{**} > \sum_{k=1, k\neq i}^u P_k^{**} + P_i^{**} > \sum_{k=1, k\neq i}^u P_k^* + P_i^* = \sum_{k=1}^u P_k^* > P'_{\max}$).

Now we have $P_i^{**} > P_i^*$ and $P_k^{**} < P_k^*$. Then $\exists \epsilon > 0$, $P_i' = P_i^{**} - \epsilon \in (P_i^*, P_i^{**})$ and $P_k' = P_k^{**} + \epsilon \in (P_k^{**}, P_k^*)$. Denote $\mathbf{P}_u' = \{P_i', P_k', \bigcup_{j\neq i, j\neq k} P_j^{**}\}$. First we have $\sum_{j=1, j\neq i, j\neq k}^u P_j^{**} + P_i' + P_k' = \sum_{j=1, j\neq i, j\neq k}^u P_j^{**} + (P_i^{**} - \epsilon) + (P_k^{**} + \epsilon) = \sum_{j=1}^u P_j^{**}$, so $\mathbf{P}_u'$ satisfies the constraint of Problem $(\mathbf{P1})$. Meanwhile, according to Proposition 1, η_i is monotonically increasing in $(0, P_i^*]$ and monotonically decreasing in (P_i^*, ∞). That means $\eta_i(P_i') > \eta_i(P_i^{**})$ and $\eta_k(P_k') > \eta_k(P_k^{**})$. As a result, $\eta(\mathbf{P}_u') = \sum_{j=1, j\neq i, j\neq k}^u \eta_j(P_j^{**}) + \eta_i(P_i') + \eta_k(P_k') > \sum_{j=1, j\neq i, j\neq k}^u \eta_j(P_j^{**}) + \eta_i(P_i^{**}) + \eta_k(P_k^{**}) = \sum_{j=1}^u \eta_j(P_j^{**}) = \eta(\mathbf{P}_u^{**})$, which contradicts with the assumption that $\mathbf{P}_u^{**}$ is the global optimum. Therefore, (22) holds. Similarly, (23) holds.

C. Proof of Proposition 2

According to Appendix I-B, η is concave when $\sum_{i=1}^u P_i^* > P'_{\max}$. We can use KKT to analyze its solution. The KKT conditions are as follows:

$$\frac{\partial \eta}{\partial P_i} + \lambda = 0, \forall i \in \{1, 2, \cdots, u\} \quad (54)$$

$$\lambda(\sum_{i=1}^u P_i - P'_{\max}) = 0 \quad (55)$$

$$\sum_{i=1}^u P_i - P'_{\max} \le 0 \quad (56)$$

$$\lambda \ge 0 \quad (57)$$

Comparing (55) and (56), if $\sum_{i=1}^u P_i - P'_{\max} < 0$, we'll have $\lambda = 0$. Then, we can obtain $\frac{\partial \eta}{\partial P_i} = 0, \forall i \in \{1, 2, \cdots, u\}$, which means the global optimum will be $\mathbf{P}_u^*$. It contradicts with the condition $\sum_{i=1}^u P_i^* > P'_{\max}$. Therefore, the global optimal will be only achieved when $\sum_{i=1}^u P_i - P'_{\max} = 0$. Proposition 2 holds.

REFERENCES

[1] 3GPP TR 25.814(V7.1.0), "Physical layer aspects for evolved universal terrestrial tadio access (UTRA)," Sept. 2006.

[2] X. Chen, H. Hu, H. Wang, H.-H. Chen, and M. Guizani, "Double proportional fair user pairing algorithm for uplink virtual MIMO systems," *IEEE Trans. Wireless Commun.*, vol. 7, no. 7, pp. 2425-2429, Jul. 2008.

[3] T. Edler and S. Lundberg, "Energy efficiency enhancements in radio access networks," in Erricsson Review, 2004.

[4] Y. Chen, S. Zhang, S. Xu, and G. Y. Li, "Fundamental trade-offs on green wireless networks," *IEEE Commun. Mag.*, vol. 49, no. 6, pp. 30-37, Jun. 2011.

[5] K. Lahiri, A. Raghunathan, S. Dey, and D. Panigrahi, "Battery-driven system design: a new frontier in low power design," in *Proc. Intl. Conf. VLSI Design*, Bangalore, India, Jan. 2002, pp. 261-267.

[6] V. Shah, N. B. Mandayam and D. J. Goodman, "Power control for wireless data based on utility and pricing," in *Proc. IEEE Personal, Indoor, Mobile Radio Comm.*, Boston, MA, Sep. 1998. pp. 1427-1432.

[7] D. J. Goodman and N. Mandayam, "Power control for wireless data," *IEEE Pers. Comm.*, vol. 7, no. 2, pp. 48-54, Apr. 2000.

[8] G. Miao, N. Himayat, and G. Li, "Energy-efficient link adaptation in frequency-selective channels," *IEEE Trans. Commun.*, vol. 58, no. 2, pp. 545-554, Feb. 2010.

[9] G. Miao, N. Himayat, G. Y. Li, S. Talwar, "Distributed interference-aware energy-efficient power optimization," *IEEE Trans. Wireless Commun.*, vol. 10, no. 4, pp. 1323-1333, Apr. 2011.

[10] S. Cui, A. J. Goldsmith, and A. Bahai, "Energy-efficiency of MIMO and cooperative MIMO techniques in sensor networks," *IEEE J. Sel. Areas Commun..*, vol. 22, no. 6, pp. 1089-1098, Aug. 2004.

[11] H. Kim, C.-B. Chae, G. de Veciana, and J. Robert W. Heath, "A cross-layer approach to energy efficiency for adaptive MIMO systems exploiting spare capacity," *IEEE Trans. Wireless Commun.*, vol. 8, no. 8, pp. 4264-4275, Aug. 2009.

[12] X. Li, M. Che, and W. Liu, "Application of STBC-encoded cooperative transmissions in wireless sensor networks," *IEEE Signal Process. Lett.*, vol. 12, no. 2, pp. 134-137, Feb. 2005.

[13] B. Bougard, G. Lenoir, A. Dejonghe, L. van der Perre, F. Catthor, and W. Dehaene, "Smart MIMO: an energy-aware adaptive MIMO-OFDM radio link control for next-generation wireless local area networks," *Eurasip J. on Wireless Commun. and Networking*, vol. 2007, no. 3, pp. 1-12, Jul. 2007.
[14] J. Zhang, M. Kountouris, J. G. Andrews, and R. W. Heath Jr., "Multi-mode transmission for the MIMO broadcast channel with imperfect channel state information," *IEEE Trans. Commun.*, vol. 59, no. 3, pp. 803-814, Mar. 2011.
[15] R. J. Muirhead, *Aspects of multivariate statistical theory*, New York: Wiely, 1982, p. 95.
[16] P. Wolniansky, G. Foschini, G. Golden, and R. Valenzuela, "V-BLAST: an architecture for realizing very high data rates over the rich-scattering wireless channel," in *Proc. Intl. Symp. on Sign., Sys., and Electr.*, Pisa, Italy, Sept. 1998, pp. 295-300.
[17] J. H. Winters , J. Salz, R. D. Gitlin, "The impact of antenna diversity on the capacity of wireless communication systems," *IEEE Trans. Commun.*, vol. 43, no. 4, pp. 1740-1751, 1994.
[18] Y. Rui, H. Hu, H. Yi, and H.-H. Chen, "A robust user pairing algorithm under channel estimation errors for uplink virtual MIMO systems," *IET Commun.*, vol. 6, no. 3, pp. 318-323, Feb. 2012.
[19] M. Alouini and A. Goldsmith, "Capacity of Rayleigh fading channels under different adaptive transmission and diversity-combining techniques, *IEEE Trans. Veh. Technol.*, vol. 48, no. 4, pp. 1165-1181, Jul. 1999.
[20] J. Zhang, J. G. Andrews, and R. W. Heath Jr., "Single-user MIMO vs. multiuser MIMO in the broadcast channel with CSIT constraints," in *Proc. IEEE Allerton Conf. on Comm. Control and Comp.*, Monticello, IL, 2008, pp. 309-314.
[21] D. Bertsekas, *Nonlinear programming*. Athena Scientific, 1999.
[22] S. Kirkpatrick, C. D. Gelatt, Jr. and M. P. Vecchi, "Optimization by simulated annealing," *Sci. Mag.*, vol. 220, no. 4598, pp. 671-680, May. 1983.
[23] V. Cerny, "Thermodynamical approach to the traveling salesman problem: an efficient simulation algorithm," *J. Optim. Theory Appl.*, vol. 45, no. 1, pp. 41-51, Jan. 1985.
[24] W. Huang, X. Wang, "Capacity scaling of general cognitive Networks," *IEEE/ACM Trans. Netw.*, vol. 20, no. 5, pp. 1501-1513, 2012.
[25] X. Wang, W. Huang, S. Wang, J. Zhang, C. Hu, "Delay and capacity tradeoff analysis for motioncast," *IEEE/ACM Trans. Netw.*, vol. 19, no. 5, pp. 1354-1367, Oct. 2011.

Yun Rui (M'11) received the B.S. degree from Southeast University (SEU) in 2004 and the Ph.D. degree from Chinese Academy of Sciences (CAS) in 2009, all in telecommunications engineering. From Feb. 2011 to Aug. 2011, he was a visiting fellow at the Department of Electronic Engineering, City University of Hong Kong. Since Sept. 2011, he has been an Associate Professor in the Shanghai Advanced Research Institute, Chinese Academy of Sciences. His research interests are in the area of broadband wireless communications, and green heterogeneous network. Dr. Rui is an Associate Editor for the WIRELESS COMMUNICATIONS AND MOBILE COMPUTING. He served as TPC members of a number of conferences, such as IEEE ICC, GlobeCom, WCNC. He also served as a TPC Co-Chair for IEEE WCNC 2013 Workshop of Convergence of Broadcast and Broadband Communication. He was a recipient of the International Conference Award of K.C. Wong Education Foundation. Dr. Rui is elected as a member of Youth Innovation Promotion Association of Chinese Academy of Sciences.

Q. T. Zhang (S'84-M'85-SM'95-F'09) received the B.Eng. from Tsinghua University, Beijing, and M.Eng. from South China University of Technology, Guangzhou, China, both in wireless communications, and the Ph.D. degree in electrical engineering from McMaster University, Hamilton, Ontario, Canada.

After graduation from McMaster in 1986, he held a research position and Adjunct Assistant Professorship at the same institution. In January 1992, he joined the Spar Aerospace Ltd., Satellite and Communication Systems Division, Montreal, as a Senior Member of Technical Staff. At Spar Aerospace, he participated in the development and manufacturing of the Radar Satellite (Radarsat). He joined Ryerson University, Toronto in 1993 and became a Professor in 1999. He then took one-year sabbatical leave at the National University of Singapore before he joined the City University in 1999, where he subsequently became a Chair Professor of Information Engineering. He is now a honorary professor with the Nanjing University of Post and Telecommunications. His research interest is on wireless communications with current focus on wireless MIMO, cooperative systems, and cognitive radio. He served as an Associate Editor for the IEEE Communications Letters from 2000 to 2007. Dr. Zhang is an IEEE Fellow.

Lei Deng received his B.S. degree in 2012 from the Department of Electronic Engineering, Shanghai Jiao Tong University, Shanghai, China. He will pursue his PH.D. degree in the Department of Information Engineering, Chinese University of Hong Kong, Hong Kong, China. His research interests are energy efficiency in wireless communication systems and large scale network optimization.

Peng Cheng received the B.S. and M.S degrees with great honors in communication and information systems from University of Electronic Science and Technology of China (UESTC), Chengdu, China, in 2006 and 2009 and the Ph.D. degree from Shanghai Jiao Tong University, Shanghai, China, in 2012. From August 2011 to August 2012, he was a Visiting Student with CSIRO ICT Center, Australia, where he is currently a Postdoctoral Research Fellow. His current research interests include cooperative communications, network MIMO, OFDM and compressed sensing theory. He is a recipient of the First Class Award of National Undergraduate Electronic Design Competition.

Mingqi Li received the Ph.D. Degree in Communication and Information Systems from Shanghai Jiaotong University in 2004 and is currently a professor and the deputy director of Research Center of Wireless Technologies for New Media, Shanghai Advanced Research Institute, Chinese Academy of Sciences. His research areas are wireless triple play, 4G/B4G key technology, and software-defined radio.